

Spin Structure Factor of the Frustrated Quantum Magnet Cs_2CuCl_4

Denis Dalidovich, Rastko Sknepnek, A. John Berlinsky,
Junhua Zhang, and Catherine Kallin

*Department of Physics and Astronomy, McMaster University,
Hamilton, Ontario, Canada L8S 4M1*

(Dated: July 18, 2018)

The ground state properties and neutron structure factor for the two-dimensional antiferromagnet on the triangular lattice, with uni-directional anisotropy in the nearest-neighbor exchange couplings and a weak Dzyaloshinskii-Moriya (DM) interaction, are studied. This Hamiltonian has been used to interpret neutron scattering measurements on the spin 1/2 spiral spin-density-wave system, Cs_2CuCl_4 , [R. Coldea, et al., Phys. Rev. B **68**, 134424 (2003)]. Calculations are performed using a $1/S$ expansion, taking into account interactions between spin-waves. The ground state energy, the shift of the ordering wave-vector, \mathbf{Q} , and the local magnetization are all calculated to order $1/S^2$. The neutron structure factor, obtained using anharmonic spin-wave Green's functions to order $1/S$, is shown to be in reasonable agreement with published neutron data, provided that slightly different parameters are used for the exchange and DM interactions than those inferred from measurements in high magnetic field.

PACS numbers: 75.10.Jm, 75.25.+z, 75.30.Ds, 75.40.Gb

I. INTRODUCTION

There is enormous interest in the condensed matter community in the possibility of observing fractionalized quasiparticles in two or three dimensional electronic systems.^{1,2,3} Fractionalization is the rule, rather than the exception, in one dimensional metals where electronic spin and charge propagate independently.⁴ Fractionally charged quasiparticles have also been found in the two dimensional electron gas in high magnetic fields where the fractional quantum Hall effect is observed.⁵ On the theoretical side, fractionalization has recently been argued to exist in frustrated two-dimensional quantum model systems,^{6,7} although no corresponding experimental systems have yet been confirmed. A set of long-wavelength theories have been developed that describe the properties of putative fractionalized magnets.^{8,9,10} Subsequently, the theoretical modeling of possible fractionalized phases was extended to a wide variety of strongly correlated electron systems.^{11,12,13} The discovery of fractionalization in real two or three dimensional systems in zero magnetic field would provide a striking example of the emergence of new kinds of particles from the collective behavior of strongly interacting electrons.¹

As a result of this intense interest, the recent claim of the observation of spinons, neutral, spin 1/2 quasiparticles, in the insulating antiferromagnet Cs_2CuCl_4 has attracted considerable attention.^{14,15} Cs_2CuCl_4 consists of nearly uncoupled layers of coupled chains. The chains are staggered, so that each spin interacts equally with two spins on each of two neighboring chains, with an antiferromagnetic coupling, J' , about 1/3 the strength of the intrachain antiferromagnetic nearest neighbor coupling, J . The layer thus resembles a triangular lattice, with strong interactions along one direction and weaker interactions in the transverse directions. These intralayer

couplings, J and J' assisted by a much weaker interlayer coupling J'' , stabilize an incommensurate spin density wave (SDW) ground state with a wave vector oriented along the chain direction. A weak Dzyaloshinskii-Moriya (DM) interaction D is believed to orient the spins in the 2D layer.

Coldea and coworkers^{14,15} used neutron scattering to study spin-wave excitations from this ordered ground state. While Coldea et al. did observe excitations similar to what is expected for spin-waves, they also saw broad features which they interpreted as excitations of pairs of spinons. Their idea is that the higher energy spin excitations resemble excitations from a nearby-lying spin-liquid state that supports fractionalized excitations. The low-dimensional nature of the system together with the low spin are argued to place this system close to a quantum critical point separating the ordered SDW state from a 2D spin liquid state. This conjecture has stimulated a number of theoretical studies of possible 2D spin-liquid states that could account for the observed behavior.^{16,17,18,19,20,21,22}

In this paper, we pursue a different interpretation of the neutron data, namely that low spin and quasi-one-dimensionality, along with non-collinear SDW order, all give rise to substantial anharmonic interactions that couple one- and two-spinwave excitations from the ordered state. The coupling to two spinwave states also yields broad spectra as seen in the neutron data. A similar conclusion has been reached by Veillette et al.,²³ who also noted that the low momentum resolution of the neutron data is another significant factor in the observed breadth of the spectra. We find that anharmonic effects lead to significant broadening of the neutron spectra but are sensitive to anisotropies, such as the DM interaction, which suppress quantum fluctuations. We show in particular that, if such anisotropies are weak, then quantum fluc-

tuations, described in terms of a $1/S$ expansion about the mean field SDW state, reduce the local moment and lead to substantial renormalizations and broadening of the excitation spectra.

The rest of this paper is organized as follows. In Sec. II we describe the Hamiltonian and the SDW state of Cs_2CuCl_4 . In Sec. III we show how anharmonic effects modify the ground state energy and the wave vector \mathbf{Q} of the SDW to order $1/S^2$, and we also review the calculation of the anharmonic one-spin-wave Green's functions to order $1/S$. In Section IV we calculate the sublattice magnetization M to order $1/S^2$ as a function of the ratio J'/J and strength of DM interaction D/J , showing that the renormalized value of M depends sensitively on the ratio D/J for small D/J . In Sec. V we examine expressions for the anharmonic spin-wave energies and damping to order $1/S$. For $D = 0$ we study how the Goldstone mode at Q is preserved and show how the preservation of this zero energy mode can be used to define a set of renormalized coupling constants. Section VI reviews the calculation of the neutron structure factor and presents a detailed comparison to the inelastic data of Coldea et al. for specific wave vectors where two-magnon scattering is important. In Sec. VII we discuss the implications of our theoretical calculations in interpreting existing data on Cs_2CuCl_4 . We also make suggestions for possible new experiments.

II. SPIN DENSITY WAVE STATE FOR Cs_2CuCl_4

The spin density wave state of Cs_2CuCl_4 can be described by the simple, model Hamiltonian for a set of decoupled layers:

$$H = \sum_{\mathbf{R}} [J\mathbf{S}_{\mathbf{R}} \cdot \mathbf{S}_{\mathbf{R}+\delta_1+\delta_2} + J'\mathbf{S}_{\mathbf{R}} \cdot (\mathbf{S}_{\mathbf{R}+\delta_1} + \mathbf{S}_{\mathbf{R}+\delta_2}) - (-1)^n \mathbf{D} \cdot \mathbf{S}_{\mathbf{R}} \times (\mathbf{S}_{\mathbf{R}+\delta_1} + \mathbf{S}_{\mathbf{R}+\delta_2})], \quad (1)$$

where J is the nearest neighbor coupling constant between $S = 1/2$ Cu^{2+} spins along chains in one direction, which we take to be the x -direction in a triangular lattice, while J' , is the coupling constant along the other two principal directions in each layer as illustrated in Fig. 1. Both J and J' are antiferromagnetic, and $J > J'$. The last term in Eq. (1) with $\mathbf{D} = (0, D, 0)$ describes the Dzyaloshinskii-Moriya interaction that alternates in sign between even and odd layers labeled by index n .

Values of the coupling constants, determined from measurements in high magnetic fields,²⁴ are:

$$J = 0.374 \text{ meV}, \quad J' = 0.128 \text{ meV} \approx J/3, \quad (2)$$

$$D = 0.02 \text{ meV}, \quad (3)$$

leading to a small Néel temperature T_N of less than 1K in the presence of the interlayer coupling J'' . The interlayer coupling is sufficiently small ($J''/J = 0.045$)²⁴ that

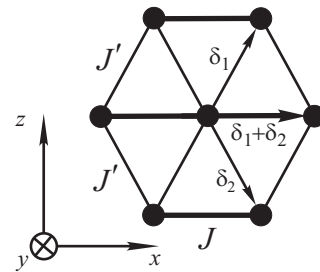


FIG. 1: Exchange couplings between the different sites of the triangular lattice within a single layer.

we neglect it in our calculations performed at $T = 0$. The classical ground state for this Hamiltonian is a SDW whose wave vector Q_0 is along the strong-coupling direction and has the value

$$Q_0 = 2\pi(0.5 + \epsilon), \quad (4)$$

where experimentally, $\epsilon = 0.030(2)$ is found for Cs_2CuCl_4 ,²⁴ so that Q_0 is close to π .

This means that individual chains are ordered approximately antiferromagnetically, while the spins in adjacent chains, which are slipped by half a lattice spacing along the chain direction, are approximately orthogonal.

To further illustrate this point, consider the calculation of the classical ground state energy of the SDW state, that can be easily determined by introducing a local reference frame, so that at every site the averaged spin is directed along the ζ axis:

$$S_{\mathbf{R}}^x = S_{\mathbf{R}}^{\xi} \cos(\mathbf{Q} \cdot \mathbf{R}) - S_{\mathbf{R}}^{\zeta} \sin(\mathbf{Q} \cdot \mathbf{R}),$$

$$S_{\mathbf{R}}^z = S_{\mathbf{R}}^{\xi} \sin(\mathbf{Q} \cdot \mathbf{R}) + S_{\mathbf{R}}^{\zeta} \cos(\mathbf{Q} \cdot \mathbf{R}),$$

$$S_{\mathbf{R}}^y = S_{\mathbf{R}}^{\eta}. \quad (5)$$

In Eqs. (5), \mathbf{Q} is the wave vector of the spiral structure, which at the classical level we write as $(Q_0, 0, 0)$ where Q_0 changes sign from layer to layer. Q_0 is determined from minimization of the classical ground state energy with $S_{\mathbf{R}}^{\xi} = S_{\mathbf{R}}^{\eta} = 0$ for all \mathbf{R} . The classical ground state energy (per spin) is given by

$$S^2 E_G^{(0)}(Q) = S^2 J_{\mathbf{Q}}^T, \quad (6)$$

$$J_{\mathbf{Q}}^T = J_{\mathbf{Q}} - iD_{\mathbf{Q}}, \quad (7)$$

where

$$J_{\mathbf{k}} = J \cos k_x + 2J' \cos \frac{k_x}{2} \cos \frac{\sqrt{3}k_y}{2}, \quad (8)$$

and

$$D_{\mathbf{k}} = -2iD \sin \frac{k_x}{2} \cos \frac{\sqrt{3}k_y}{2} \quad (9)$$

are the Fourier transforms of the exchange and DM interactions of the Hamiltonian respectively.

For $D = 0$, ϵ in Eq. (4) is given by

$$\epsilon = \frac{1}{\pi} \arcsin\left(\frac{J'}{2J}\right) = 0.0547, \quad (10)$$

while for $D = 0.02$ meV, the value of Q_0 that minimizes the classical ground state energy corresponds to $\epsilon = 0.0533$ for the experimental values of J and J' . The two terms in Eq. (8), represent the intrachain and interchain energies respectively. Substituting the actual value of Q_0 for a given J'/J and $D = 0$, we find that

$$S^2 E_G^{(0)}(Q_0) = -JS^2 \left[1 + \frac{J'^2}{2J^2}\right]. \quad (11)$$

Thus the contribution to the ground state energy from the interchain coupling is of order $(J')^2/J^2$ compared to the intrachain contribution. Quantum fluctuations reduce the effectiveness of interchain coupling further by renormalizing the SDW wave vector to a value even closer to π (corresponding to a smaller effective J'/J). At the same time, quantum fluctuations lower the total energy. Thus if one were to model the effects of quantum fluctuations in terms of effective coupling constants, \tilde{J} and \tilde{J}' , the result would be $\tilde{J}'/\tilde{J} < J'/J$ and $\tilde{J} > J$. As is shown in the next section and in Appendix A, the value of ϵ obtained at the classical level, is in fact considerably renormalized by quantum fluctuations.

III. 1/S EXPANSION

To address the physics determined by quantum fluctuations, we employ the well-known Holstein-Primakoff transformation for the spin operators:²⁵

$$S_{\mathbf{R}}^- = S_{\mathbf{R}}^\xi - iS_{\mathbf{R}}^\eta \approx \sqrt{2S} a_{\mathbf{R}}^\dagger \left[1 - \frac{1}{4S} a_{\mathbf{R}}^\dagger a_{\mathbf{R}}\right], \quad (12)$$

$$S_{\mathbf{R}}^+ = S_{\mathbf{R}}^\xi + iS_{\mathbf{R}}^\eta \approx \sqrt{2S} \left[1 - \frac{1}{4S} a_{\mathbf{R}}^\dagger a_{\mathbf{R}}\right] a_{\mathbf{R}}, \quad (13)$$

$$\mathcal{H}^{(4)} = \frac{1}{4N} \sum_{\mathbf{1}, \mathbf{2}, \mathbf{3}, \mathbf{4}} \left\{ [(A_{\mathbf{1}-\mathbf{3}} + A_{\mathbf{1}-\mathbf{4}} + A_{\mathbf{2}-\mathbf{3}} + A_{\mathbf{2}-\mathbf{4}}) - (B_{\mathbf{1}-\mathbf{3}} + B_{\mathbf{1}-\mathbf{4}} + B_{\mathbf{2}-\mathbf{3}} + B_{\mathbf{2}-\mathbf{4}}) - (A_{\mathbf{1}} + A_{\mathbf{2}} + A_{\mathbf{3}} + A_{\mathbf{4}})] \right. \\ \left. a_{\mathbf{1}}^\dagger a_{\mathbf{2}}^\dagger a_{\mathbf{3}} a_{\mathbf{4}} \delta_{\mathbf{1}+\mathbf{2}, \mathbf{3}+\mathbf{4}} + \frac{2}{3} (B_{\mathbf{1}} + B_{\mathbf{2}} + B_{\mathbf{3}}) (a_{\mathbf{1}}^\dagger a_{\mathbf{2}}^\dagger a_{\mathbf{3}}^\dagger a_{\mathbf{4}} + a_{\mathbf{4}}^\dagger a_{\mathbf{3}} a_{\mathbf{2}} a_{\mathbf{1}}) \delta_{\mathbf{1}+\mathbf{2}+\mathbf{3}, \mathbf{4}} \right\}, \quad (21)$$

and contains only symmetric vertices. It is important to emphasize that $\mathcal{H}^{(3)}$ comes from the coupling between the operators $S_{\mathbf{R}}^\xi$ and $S_{\mathbf{R}}^\zeta$, which arises for non-collinear ordered states. This term plays a crucial role in calcula-

$$S_{\mathbf{R}}^\zeta = S - a_{\mathbf{R}}^\dagger a_{\mathbf{R}}. \quad (14)$$

These are written in a form with the square root expanded to first order in $1/(2S)$. The magnon operators $a_{\mathbf{R}}^\dagger$, $a_{\mathbf{R}}$ describe excitations around the spiral ground state and obey Bose statistics. Substituting the transformations (12)-(14) into Eq. (1), we obtain the Hamiltonian for interacting magnons,

$$\mathcal{H} = S^2 E_G^{(0)}(Q) + (\mathcal{H}^{(2)} + \mathcal{H}^{(3)} + \mathcal{H}^{(4)}), \quad (15)$$

where in the Fourier transformed representation

$$\mathcal{H}^{(2)} = 2S \sum_{\mathbf{k}} \left(A_{\mathbf{k}} a_{\mathbf{k}}^\dagger a_{\mathbf{k}} - \frac{B_{\mathbf{k}}}{2} (a_{\mathbf{k}}^\dagger a_{-\mathbf{k}}^\dagger + a_{\mathbf{k}} a_{-\mathbf{k}}) \right). \quad (16)$$

The functions $A_{\mathbf{k}}$ and $B_{\mathbf{k}}$ are expressed through $J_{\mathbf{k}}$ as

$$A_{\mathbf{k}} = \frac{1}{4} [J_{\mathbf{Q}+\mathbf{k}}^T + J_{\mathbf{Q}-\mathbf{k}}^T] + \frac{J_{\mathbf{k}}}{2} - J_{\mathbf{Q}}^T, \quad (17)$$

$$B_{\mathbf{k}} = \frac{J_{\mathbf{k}}}{2} - \frac{1}{4} [J_{\mathbf{Q}+\mathbf{k}}^T + J_{\mathbf{Q}-\mathbf{k}}^T]. \quad (18)$$

The interactions between magnons are described by the last two terms $\mathcal{H}^{(3)}$ and $\mathcal{H}^{(4)}$. The three-magnon term can be written in the form

$$\mathcal{H}^{(3)} = \frac{i}{2} \sqrt{\frac{S}{2N}} \sum_{\mathbf{1}, \mathbf{2}, \mathbf{3}} (C_{\mathbf{1}} + C_{\mathbf{2}}) (a_{\mathbf{3}}^\dagger a_{\mathbf{2}} a_{\mathbf{1}} - a_{\mathbf{1}}^\dagger a_{\mathbf{2}}^\dagger a_{\mathbf{3}}) \delta_{\mathbf{1}+\mathbf{2}, \mathbf{3}} \quad (19)$$

that contains the vertex

$$C_{\mathbf{k}} = (J_{\mathbf{Q}+\mathbf{k}}^T - J_{\mathbf{Q}-\mathbf{k}}^T), \quad (20)$$

which is antisymmetric with respect to the transformation $\mathbf{k} \rightarrow -\mathbf{k}$. For brevity, in longer expressions we use the convention that $\mathbf{1} = \mathbf{k}_1$, etc.

The four-magnon term can be conveniently written as:

tions of the structure factor as well as in renormalization of the energy spectrum.

To proceed, one needs to diagonalize the quadratic part of the Hamiltonian Eq. (16) by means of the Bogoliubov

transformation:

$$a_{\mathbf{k}} = u_{\mathbf{k}}c_{\mathbf{k}} + v_{\mathbf{k}}c_{-\mathbf{k}}^{\dagger}, \quad a_{-\mathbf{k}}^{\dagger} = u_{\mathbf{k}}c_{-\mathbf{k}}^{\dagger} + v_{\mathbf{k}}c_{\mathbf{k}}, \quad (22)$$

$$u_{\mathbf{k}} = \sqrt{\frac{A_{\mathbf{k}} + \varepsilon_{\mathbf{k}}}{2\varepsilon_{\mathbf{k}}}}, \quad v_{\mathbf{k}} = \text{sgn}B_{\mathbf{k}}\sqrt{\frac{A_{\mathbf{k}} - \varepsilon_{\mathbf{k}}}{2\varepsilon_{\mathbf{k}}}}. \quad (23)$$

The energy spectrum in the above equations is given by:

$$\begin{aligned} \varepsilon_{\mathbf{k}} &= \sqrt{A_{\mathbf{k}}^2 - B_{\mathbf{k}}^2} \\ &= \sqrt{(J_{\mathbf{k}} - J_{\mathbf{Q}}^T) \left[(J_{\mathbf{Q}+\mathbf{k}}^T + J_{\mathbf{Q}-\mathbf{k}}^T)/2 - J_{\mathbf{Q}}^T \right]}. \end{aligned} \quad (24)$$

For $D = 0$, the magnon spectrum has zeros at $\mathbf{k} = 0$ and $\mathbf{k} = \pm\mathbf{Q}$ in the two-dimensional Brillouin zone, while a non-zero D leads to the appearance of a finite gap of order \sqrt{DJ} around the \mathbf{Q} -points. After diagonalization, $\mathcal{H}^{(2)}$ takes the form:

$$\mathcal{H}^{(2)} = SE_G^{(1)}(Q) + \frac{2S}{N} \sum_{\mathbf{k}} \varepsilon_{\mathbf{k}} c_{\mathbf{k}}^{\dagger} c_{\mathbf{k}}, \quad (25)$$

$$E_G^{(1)}(Q) = J_{\mathbf{Q}}^T + \frac{1}{N} \sum_{\mathbf{k}} \varepsilon_{\mathbf{k}}. \quad (26)$$

The contribution $SE_G^{(1)}(Q)$ gives the leading $1/(2S)$ correction to the classical ground state energy Eq. (6). Minimizing the sum $S^2E_G^{(0)}(Q) + SE_G^{(1)}(Q)$, we find the quantum correction to the classical value Q_0 . To order $1/S$ the shifted wave vector is $\mathbf{Q} = (Q, 0, 0)$

$$Q = Q_0 + \frac{\Delta Q^{(1)}}{2S}, \quad (27)$$

$$\Delta Q^{(1)} = - \left[\frac{\partial^2 J_{\mathbf{Q}}^T}{\partial Q^2} \right]^{-1} \frac{1}{N} \sum_{\mathbf{k}} \frac{(A_{\mathbf{k}} + B_{\mathbf{k}})}{\varepsilon_{\mathbf{k}}} \cdot \frac{\partial J_{\mathbf{Q}+\mathbf{k}}^T}{\partial Q} \Big|_{Q_0} \quad (28)$$

In the absence of the DM interaction,

$$\Delta Q^{(1)}/2\pi = -0.0324, \quad (29)$$

while for $D = 0.02$ meV,

$$\Delta Q^{(1)}/2\pi = -0.0228. \quad (30)$$

We see that inclusion of the Dzyaloshinskii-Moriya interaction suppresses the renormalization of Q towards π .

It is possible to go further and also calculate the correction to the ground state energy and the ordering wave vector Q that is of order $1/(2S)^2$. The details of those calculations are presented in Appendix A. The results indicate that quantum corrections computed order by order in $1/(2S)$ are significant for the values of J and J' given by Eqs. (2). To further explore this issue, one can compare the classical ground state energy Eq. (6) to its leading renormalization due to quantum fluctuations $SE_G^{(1)}(Q_0)$. We find, for $D = 0$

$$S^2E_G^{(0)}(Q_0)/J = -0.265, \quad SE_G^{(1)}(Q_0)/J = -0.157, \quad (31)$$

and, for $D = 0.02$ meV,

$$S^2E_G^{(0)}(Q_0)/J = -0.291, \quad SE_G^{(1)}(Q_0)/J = -0.138. \quad (32)$$

We see that the leading quantum correction lowers the ground state energy by about 50%, giving reasonable agreement with a recent experimental determination of this quantity, based on susceptibility measurements,²⁶ which yields a ground state energy slightly above $-0.5J$. We show in Appendix A that for $D = 0$ the next order in $1/(2S)$ correction reduces the ground state energy by a further 10 percent below the sum of the values given in Eq. (31), bringing the total within a few percent of the experimental value.

To calculate physical observables, we need the Green's functions for the magnon operators $a_{\mathbf{k}}$. They can be conveniently written in the form of a 2×2 matrix, indicating the presence of normal and anomalous parts. At zero temperature, the definition reads

$$i\hat{G}(\mathbf{k}, \omega) = \int_{-\infty}^{\infty} dt e^{i\omega t} \left\langle \hat{T} \begin{bmatrix} a_{\mathbf{k}}(t) \\ a_{-\mathbf{k}}^{\dagger}(t) \end{bmatrix} \begin{bmatrix} a_{\mathbf{k}}^{\dagger}(0) a_{-\mathbf{k}}(0) \end{bmatrix} \right\rangle, \quad (33)$$

where \hat{T} is the time ordering operator, and the average is taken with respect to the ground state. The inverse of the matrix for the bare Green's functions has the form²⁹

$$\hat{G}^{(0)-1}(\mathbf{k}, \omega) = \begin{pmatrix} \omega - 2SA_{\mathbf{k}} + i\eta & 2SB_{\mathbf{k}} \\ 2SB_{\mathbf{k}} & -\omega - 2SA_{\mathbf{k}} + i\eta \end{pmatrix}, \quad (34)$$

corresponding to the Green's function

$$\hat{G}^{(0)}(\mathbf{k}, \omega) = \frac{1}{(\omega - \omega_{\mathbf{k}} + i\eta)(\omega + \omega_{\mathbf{k}} - i\eta)} \begin{pmatrix} \omega + 2SA_{\mathbf{k}} - i\eta & 2SB_{\mathbf{k}} \\ 2SB_{\mathbf{k}} & -\omega + 2SA_{\mathbf{k}} - i\eta \end{pmatrix}, \quad (35)$$

where $\omega_{\mathbf{k}} = 2S\varepsilon_{\mathbf{k}}$. The self-energy $\hat{\Sigma}(\mathbf{k}, \omega)$ determining the exact Green's function is also a 2×2 matrix, that can be parametrized as

$$\hat{\Sigma}(\mathbf{k}, \omega) = \begin{pmatrix} X(\mathbf{k}, \omega) + Y(\mathbf{k}, \omega) & Z(\mathbf{k}, \omega) \\ Z(\mathbf{k}, \omega) & X(\mathbf{k}, \omega) - Y(\mathbf{k}, \omega) \end{pmatrix}, \quad (36)$$

and which satisfies the Dyson equation

$$\hat{G}^{-1}(\mathbf{k}, \omega) = \hat{G}^{(0)-1}(\mathbf{k}, \omega) - \hat{\Sigma}(\mathbf{k}, \omega). \quad (37)$$

The self-energy to order $1/(2S)$ consists of two parts

$$\hat{\Sigma}(\mathbf{k}, \omega) = \hat{\Sigma}^{(4)}(\mathbf{k}) + \hat{\Sigma}^{(3)}(\mathbf{k}, \omega). \quad (38)$$

The contribution $\hat{\Sigma}^{(4)}(\mathbf{k})$ is frequency independent and can be calculated simply by the Hartree-Fock decoupling of the quartic term in the Hamiltonian Eq. (21).

$$X^{(4)}(\mathbf{k}) = A_{\mathbf{k}} + \frac{2S}{N} \sum_{\mathbf{q}} \frac{1}{\omega_{\mathbf{q}}} \left[\left(\frac{1}{2} B_{\mathbf{k}} + B_{\mathbf{q}} \right) B_{\mathbf{q}} + (A_{\mathbf{k}-\mathbf{q}} - B_{\mathbf{k}-\mathbf{q}} - A_{\mathbf{q}} - A_{\mathbf{k}}) A_{\mathbf{q}} \right], \quad (39)$$

$$Y^{(4)}(\mathbf{k}) = -B_{\mathbf{k}} + \frac{2S}{N} \sum_{\mathbf{q}} \frac{1}{\omega_{\mathbf{q}}} \left[(B_{\mathbf{k}} + B_{\mathbf{q}}) A_{\mathbf{q}} + \left(A_{\mathbf{k}-\mathbf{q}} - B_{\mathbf{k}-\mathbf{q}} - A_{\mathbf{q}} - \frac{1}{2} A_{\mathbf{k}} \right) B_{\mathbf{q}} \right], \quad (40)$$

$$Z^{(4)}(\mathbf{k}) = 0. \quad (41)$$

$\hat{\Sigma}^{(3)}(\mathbf{k}, \omega)$ is the contribution arising from the three-magnon interactions, $\mathcal{H}^{(3)}$. Its non-zero imaginary part determines the magnon damping to first order in $1/(2S)$. The corresponding components are most easily calculated by transforming Eq. (19) to the $c_{\mathbf{k}}$ -operator basis using the Bogoliubov transformations, Eqs. (22).

$$X^{(3)}(\mathbf{k}, \omega) = -\frac{S}{16N} \sum_{\mathbf{q}} \left\{ [\Phi_1(\mathbf{q}, \mathbf{k} - \mathbf{q})]^2 + [\Phi_2(\mathbf{q}, \mathbf{k} - \mathbf{q})]^2 \right\} \left(\frac{1}{\omega_{\mathbf{q}} + \omega_{\mathbf{k}-\mathbf{q}} - \omega - i\eta} + \frac{1}{\omega_{\mathbf{q}} + \omega_{\mathbf{k}-\mathbf{q}} + \omega - i\eta} \right),$$

$$Z^{(3)}(\mathbf{k}, \omega) = -\frac{S}{16N} \sum_{\mathbf{q}} \left\{ [\Phi_1(\mathbf{q}, \mathbf{k} - \mathbf{q})]^2 - [\Phi_2(\mathbf{q}, \mathbf{k} - \mathbf{q})]^2 \right\} \left(\frac{1}{\omega_{\mathbf{q}} + \omega_{\mathbf{k}-\mathbf{q}} - \omega - i\eta} + \frac{1}{\omega_{\mathbf{q}} + \omega_{\mathbf{k}-\mathbf{q}} + \omega - i\eta} \right),$$

$$Y^{(3)}(\mathbf{k}, \omega) = -\frac{S}{16N} \sum_{\mathbf{q}} \{ 2\Phi_1(\mathbf{q}, \mathbf{k} - \mathbf{q})\Phi_2(\mathbf{q}, \mathbf{k} - \mathbf{q}) \} \left(\frac{1}{\omega_{\mathbf{q}} + \omega_{\mathbf{k}-\mathbf{q}} - \omega - i\eta} - \frac{1}{\omega_{\mathbf{q}} + \omega_{\mathbf{k}-\mathbf{q}} + \omega - i\eta} \right). \quad (42)$$

$$\begin{aligned} \Phi_1(\mathbf{q}, \mathbf{k} - \mathbf{q}) &= (C_{\mathbf{q}} + C_{\mathbf{k}-\mathbf{q}}) (u_{\mathbf{q}} + v_{\mathbf{q}}) (u_{\mathbf{k}-\mathbf{q}} + v_{\mathbf{k}-\mathbf{q}}) - 2C_{\mathbf{k}} (u_{\mathbf{q}} v_{\mathbf{k}-\mathbf{q}} + v_{\mathbf{q}} u_{\mathbf{k}-\mathbf{q}}), \\ \Phi_2(\mathbf{q}, \mathbf{k} - \mathbf{q}) &= C_{\mathbf{q}} (u_{\mathbf{q}} + v_{\mathbf{q}}) (u_{\mathbf{k}-\mathbf{q}} - v_{\mathbf{k}-\mathbf{q}}) + C_{\mathbf{k}-\mathbf{q}} (u_{\mathbf{k}-\mathbf{q}} + v_{\mathbf{k}-\mathbf{q}}) (u_{\mathbf{q}} - v_{\mathbf{q}}). \end{aligned} \quad (43)$$

IV. SUBLATTICE MAGNETIZATION

In this section we consider the staggered magnetization for a range of values of J'/J and D/J and show that quantum fluctuations lead to a considerable renormalization of the average value of the local moment. From the operator definition Eq. (14) we can write the staggered magnetization as

$$M = S + \frac{1}{N} \sum_{\mathbf{k}} \int \frac{d\omega}{2\pi i} G_{11}(\mathbf{k}, \omega) e^{-i\omega 0_-}, \quad (44)$$

where the exact Green's function $G_{11}(\mathbf{k}, \omega)$ is the corresponding element of the full matrix $\hat{G}(\mathbf{k}, \omega)$ and 0_- is a negative infinitesimal. To lowest order in $1/(2S)$, one can use $G_{11}^{(0)}(\mathbf{k}, \omega)$ of Eq. (35), to find the first order correction to the $S = 1/2$ value

$$\Delta M^{(1)} = -\frac{1}{2N} \sum_{\mathbf{k}} \left(\frac{A_{\mathbf{k}}}{\varepsilon_{\mathbf{k}}} - 1 \right). \quad (45)$$

For the next order correction in $1/(2S)$, there are two contributions. The first one, denoted as $\Delta M_1^{(2)}$, arises from renormalization by quantum fluctuations of the ordering wave vector Q_0 . This correction is obtainable by

substituting the renormalized value Q given by Eq. (27) into the formula above and expanding using Eq. (45) up to first order in $1/(2S)$.

$$\Delta M_I^{(2)} = \frac{\Delta Q^{(1)}}{2S} \frac{1}{N} \sum_{\mathbf{k}} \frac{B_{\mathbf{k}}(A_{\mathbf{k}} + B_{\mathbf{k}})}{4\varepsilon_{\mathbf{k}}^3} \cdot \left. \frac{\partial J_{\mathbf{Q}+\mathbf{k}}^T}{\partial Q} \right|_{Q_0}. \quad (46)$$

The second contribution is determined by the self-energy corrections of order $1/(2S)$ to the Green's function itself and is given by

$$\Delta M_{II}^{(2)} = \frac{1}{N} \sum_{\mathbf{k}} \int \frac{d\omega}{2\pi i} e^{-i\omega_0} \Delta \hat{G}_{11}(\mathbf{k}, \omega), \quad (47)$$

where

$$\Delta G_{11}(\mathbf{k}, \omega) = \left(\hat{G}^{(0)}(\mathbf{k}, \omega) \hat{\Sigma}(\mathbf{k}, \omega) \hat{G}^{(0)}(\mathbf{k}, \omega) \right)_{11} = [X(\mathbf{k}, \omega) + Y(\mathbf{k}, \omega)] \left[G_{11}^{(0)}(\mathbf{k}, \omega) \right]^2 + 2Z(\mathbf{k}, \omega) G_{11}^{(0)}(\mathbf{k}, \omega) G_{12}^{(0)}(\mathbf{k}, \omega) + [X(\mathbf{k}, \omega) - Y(\mathbf{k}, \omega)] \left[G_{12}^{(0)}(\mathbf{k}, \omega) \right]^2. \quad (48)$$

This correction, as a result of integration over ω , will contain two parts, so that

$$\Delta M_{II}^{(2)} = \Delta M_a^{(2)} + \Delta M_b^{(2)}. \quad (49)$$

One part comes from taking the residues at the poles of self-energies, while the other results from the double-poles of the products of two Green's functions. Using Eqs. (39)-(42), we obtain the first contribution

$$\Delta M_a^{(2)} = -\frac{S}{8N} \sum_{\mathbf{k}, \mathbf{q}} \left\{ \frac{[\Phi_1(\mathbf{q}, \mathbf{k} - \mathbf{q})]^2}{2} \left[G_{11}^{(0)}(\mathbf{k}, \Omega_{\mathbf{k}, \mathbf{q}}) + G_{12}^{(0)}(\mathbf{k}, \Omega_{\mathbf{k}, \mathbf{q}}) \right]^2 + \frac{[\Phi_2(\mathbf{q}, \mathbf{k} - \mathbf{q})]^2}{2} \left[G_{11}^{(0)}(\mathbf{k}, \Omega_{\mathbf{k}, \mathbf{q}}) - G_{12}^{(0)}(\mathbf{k}, \Omega_{\mathbf{k}, \mathbf{q}}) \right]^2 - \Phi_1(\mathbf{q}, \mathbf{k} - \mathbf{q}) \Phi_2(\mathbf{q}, \mathbf{k} - \mathbf{q}) \left[\left[G_{11}^{(0)}(\mathbf{k}, \Omega_{\mathbf{k}, \mathbf{q}}) \right]^2 - \left[G_{12}^{(0)}(\mathbf{k}, \Omega_{\mathbf{k}, \mathbf{q}}) \right]^2 \right] \right\}, \quad (50)$$

$$\Omega_{\mathbf{k}, \mathbf{q}} = -\omega_{\mathbf{q}} - \omega_{\mathbf{k} - \mathbf{q}}. \quad (51)$$

The contribution arising from the residues at the double-poles of the products of two Green's functions in Eqs. (47)-(48), is straightforward to calculate as well. After some algebra, we find that

$$\Delta M_b^{(2)} = \frac{1}{2SN} \sum_{\mathbf{k}} \frac{B_{\mathbf{k}}}{4\varepsilon_{\mathbf{k}}^3} \left\{ [X(\mathbf{k}, \omega_{\mathbf{k}}) + Z(\mathbf{k}, \omega_{\mathbf{k}})] [A_{\mathbf{k}} + B_{\mathbf{k}}] - [X(\mathbf{k}, \omega_{\mathbf{k}}) - Z(\mathbf{k}, \omega_{\mathbf{k}})] [A_{\mathbf{k}} - B_{\mathbf{k}}] \right\} + \frac{1}{N} \sum_{\mathbf{k}} \frac{(A_{\mathbf{k}} - \varepsilon_{\mathbf{k}})}{4\varepsilon_{\mathbf{k}}^2} \left\{ [X'(\mathbf{k}, \omega_{\mathbf{k}}) + Z'(\mathbf{k}, \omega_{\mathbf{k}})] [A_{\mathbf{k}} + B_{\mathbf{k}}] - [X'(\mathbf{k}, \omega_{\mathbf{k}}) - Z'(\mathbf{k}, \omega_{\mathbf{k}})] [A_{\mathbf{k}} - B_{\mathbf{k}}] - 2Y'(\mathbf{k}, \omega_{\mathbf{k}}) \varepsilon_{\mathbf{k}} \right\}, \quad (52)$$

where $\omega_{\mathbf{k}} = 2S\varepsilon_{\mathbf{k}}$, and

$$\left\{ X'(\mathbf{k}, \omega_{\mathbf{k}}), Y'(\mathbf{k}, \omega_{\mathbf{k}}), Z'(\mathbf{k}, \omega_{\mathbf{k}}) \right\} = \left\{ \frac{\partial X(\mathbf{k}, \omega)}{\partial \omega}, \frac{\partial Y(\mathbf{k}, \omega)}{\partial \omega}, \frac{\partial Z(\mathbf{k}, \omega)}{\partial \omega} \right\} \Big|_{\omega=\omega_{\mathbf{k}}}. \quad (53)$$

It is clear from the expressions above that both $\Delta M_I^{(2)}$ and $\Delta M_{II}^{(2)}$ contain the overall prefactor $1/(2S)$.

In Fig. 2, we plot the total sublattice magnetization

$$M = S + \Delta M^{(1)} + \Delta M_I^{(2)} + \Delta M_{II}^{(2)} \quad (54)$$

as a function of Dzyaloshinskii-Moriya interaction D , for coupling constants J and J' as given by Eqs. (2). The

ratios of each correction to the classical magnetization $S = 1/2$, $-\Delta M/S$, are also plotted, as explained in the caption of Fig. 2. One can see that the renormalization of the local magnetization by quantum fluctuations to second order in $1/(2S)$ is considerable for all values of D between 0 and 0.025 meV, although increasing D clearly suppresses fluctuations making the system more classical. The figure also shows a calculated sublattice magnetiza-

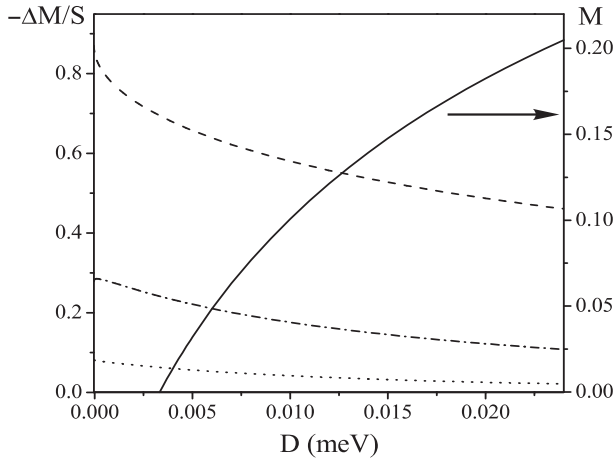


FIG. 2: The total value of sublattice magnetization M , Eq. (54), calculated up to the second order in $1/(2S)$ as a function of Dzyaloshinskii-Moriya interaction D , is shown by the solid line. The dashed, dotted and dashed-dotted lines are the results for the quantum corrections $-\Delta M^{(1)}$, $-\Delta M_I^{(2)}$ and $-\Delta M_{II}^{(2)}$, respectively, divided by $S = 1/2$.

tion that is negative for D between 0 and $D \approx 0.003$

meV, signaling the melting of the assumed spiral ordered ground state by quantum fluctuations when D is too small.

Experimentally, a value of $-\Delta M/S \approx 0.25$ was inferred by Coldea and co-workers³¹ from elastic neutron scattering, and this value was used in the analysis of the most recent neutron data.¹⁴ Such a small renormalization of the local moment is incompatible with the theory presented here. It is also unlikely to be explained by the addition of the very small expected interlayer exchange coupling $J''/J = 0.045$.^{14,24} It is indeed puzzling that such a small moment reduction, which is less than for the spin 1/2 Heisenberg antiferromagnet on a two-dimensional square lattice, would occur in this system which is both frustrated and close to the one-dimensional limit.

V. ENERGY SPECTRUM

The renormalized magnon energy spectrum $\tilde{\omega}_{\mathbf{k}} = 2S\tilde{\epsilon}_{\mathbf{k}}$ can be found from the poles of the exact Green's function, determined by²⁹

$$\text{Re} \left\{ \det \hat{G}^{-1}(\mathbf{k}, \tilde{\omega}_{\mathbf{k}}) \right\} = \text{Re} \left\{ \det \left[\hat{G}^{(0)-1}(\mathbf{k}, \tilde{\omega}_{\mathbf{k}}) - \hat{\Sigma}(\mathbf{k}, \tilde{\omega}_{\mathbf{k}}) \right] \right\} = 0, \quad (55)$$

which leads to the self-consistency equation:

$$\begin{aligned} \tilde{\omega}_{\mathbf{k}} = & \left\{ \{2S(A_{\mathbf{k}} + B_{\mathbf{k}}) + \text{Re}[X(\mathbf{k}, \tilde{\omega}_{\mathbf{k}}) - Z(\mathbf{k}, \tilde{\omega}_{\mathbf{k}})]\} \{2S(A_{\mathbf{k}} - B_{\mathbf{k}}) + \text{Re}[X(\mathbf{k}, \tilde{\omega}_{\mathbf{k}}) + Z(\mathbf{k}, \tilde{\omega}_{\mathbf{k}})]\} \right. \\ & \left. - \{\text{Im}[X(\mathbf{k}, \tilde{\omega}_{\mathbf{k}}) + Z(\mathbf{k}, \tilde{\omega}_{\mathbf{k}})]\} \{\text{Im}[X(\mathbf{k}, \tilde{\omega}_{\mathbf{k}}) - Z(\mathbf{k}, \tilde{\omega}_{\mathbf{k}})]\} + [\text{Im}Y(\mathbf{k}, \tilde{\omega}_{\mathbf{k}})]^2 \right\}^{1/2} + \text{Re}Y(\mathbf{k}, \tilde{\omega}_{\mathbf{k}}). \end{aligned} \quad (56)$$

Near these poles, if the imaginary part of the self-energy is small, the shape of the one-magnon spectrum is approximately Lorentzian and has the form²⁹

$$\det \hat{G}^{-1}(\mathbf{k}, \omega) \simeq -2\omega_{\mathbf{k}}z_{\mathbf{k}}(\omega - \tilde{\omega}_{\mathbf{k}}) + i\text{Im} \left[\det \hat{G}^{-1}(\mathbf{k}, \tilde{\omega}_{\mathbf{k}}) \right], \quad (57)$$

where

$$2\omega_{\mathbf{k}}z_{\mathbf{k}} = -\frac{\partial}{\partial \omega} \text{Re} \left[\det \hat{G}^{-1}(\mathbf{k}, \omega) \right] \Big|_{\omega=\tilde{\omega}_{\mathbf{k}}}. \quad (58)$$

The imaginary part of Eq. (57) determines the inverse life-time of the quasiparticles. To calculate the half-width at half-maximum of the peak, we use the parameter

$$\Gamma_{\mathbf{k}} \simeq \frac{|\text{Im}[\det \hat{G}^{-1}(\mathbf{k}, \tilde{\omega}_{\mathbf{k}})]|}{2\omega_{\mathbf{k}}z_{\mathbf{k}}}. \quad (59)$$

Equation (56), although formally exact, implicitly includes contributions of all orders in $1/S$. Furthermore,

quantities such as the terms $2S(A_{\mathbf{k}} \pm B_{\mathbf{k}})$ that are of the leading order in S , should be corrected for the first order shift of the ordering wave vector from \mathbf{Q}_0 to \mathbf{Q} , given by Eqs. (27)-(28). Although the self-energies are only calculated to order $1/S$, taking the square root of a sum of squares of self-energies evaluated at renormalized frequencies, effectively mixes in higher order corrections. Also, particularly for the case $D = 0$, there is cancellation among terms of order $1/S$, leaving a result, at the shifted Q -vector, which is the square root of residual $1/S^2$ terms, which may be negative.

A simple way to preserve physical behavior at the Goldstone wave vector \mathbf{Q} for $D = 0$, is to evaluate the

self-energies using renormalized coupling constants, for which the classical ordering wave vector is \mathbf{Q} , that is

$$Q = \pi + 2 \arcsin \left(\frac{\bar{J}'}{2\bar{J}} \right). \quad (60)$$

The effect of this renormalization, which determines the ratio \bar{J}'/\bar{J} and represents a higher order in $1/S$ correction to the self-energies, is that the self-energies will vanish at the renormalized \mathbf{Q} . A further renormalization of \bar{J} by itself is defined by the condition that the coefficient of the linear term in $|\mathbf{k} - \mathbf{Q}|$ inside the square root vanishes for $\mathbf{k} = \mathbf{Q}$, so that the energy dispersion relation around this point is linear in $|\mathbf{k} - \mathbf{Q}|$. The procedure of expanding the self-energies around \mathbf{Q} is tedious but completely equivalent to that described elsewhere.^{29,30} Omitting the intermediate steps, we obtain the condition

$$\left. \frac{\partial J_{\mathbf{k}}}{\partial \mathbf{k}} \right|_{\mathbf{k}=\mathbf{Q}} = -\frac{1}{2SN} \sum_{\mathbf{p}} \frac{(\bar{A}_{\mathbf{p}} + \bar{B}_{\mathbf{p}})}{\bar{\varepsilon}_{\mathbf{p}}} \cdot \frac{\partial \bar{J}_{\mathbf{p}+\mathbf{Q}}}{\partial \mathbf{p}}, \quad (61)$$

where the bars indicate that the renormalized values \bar{J} and \bar{J}' should be used in the right hand side of this equation. One can easily check that, within this approach, we retain consistency up to lowest order in $1/2S$. Indeed, expanding the derivative $\partial J_{\mathbf{k}}/\partial \mathbf{k}$ around Q_0 , we recover Eq. (28) for the correction to the ordering wave vector. Using Eqs. (2), we find from Eqs. (60)-(61) that

$$\bar{J} \approx 0.472 \text{ meV}, \quad \bar{J}' \approx 0.066 \text{ meV}. \quad (62)$$

We see that in this approach, J' is renormalized down from its bare value, while J increases, as discussed in Sec. II.

In spite of the fact that we expect the system to be unstable for $D = 0$ and $J'/J = 1/3$, it is of pedagogical interest to examine the effects of anharmonicity and the shift of the Goldstone mode for this case. The right hand panel of Fig. 3 shows the results for the renormalized energy spectrum and its comparison to the linear spin-wave dispersion along the $(1,0)$ direction for $D = 0$. The inverse lifetime of quasiparticles Eq. (59) is also shown. The excitations are seen to be heavily overdamped close to the (10) point. Also kinks are seen at various places in the renormalized curves, apparently at points where one-to-two magnon decay channels turn on. Although not shown in Fig. 3, we also find that the band width of the dispersion along $(1,0) \rightarrow (1,1)$ is renormalized downward by about a factor of 3 due to anharmonic effects.

In the left hand panel of Fig. 3, we plot the renormalized energy spectrum for $D = 0.02$ meV.²³ In the presence of this DM interaction, it suffices to use the bare values for the coupling constants in expressions for self-energies, since the finite gap in the spectrum does not lead to any problematic behavior near \mathbf{Q} when D is not too small. The effects of quantum fluctuations are very sensitive to the presence of a non-zero D . Increasing the value of D reduces the interaction-induced damping of quasiparticles, making them more stable. Quantum

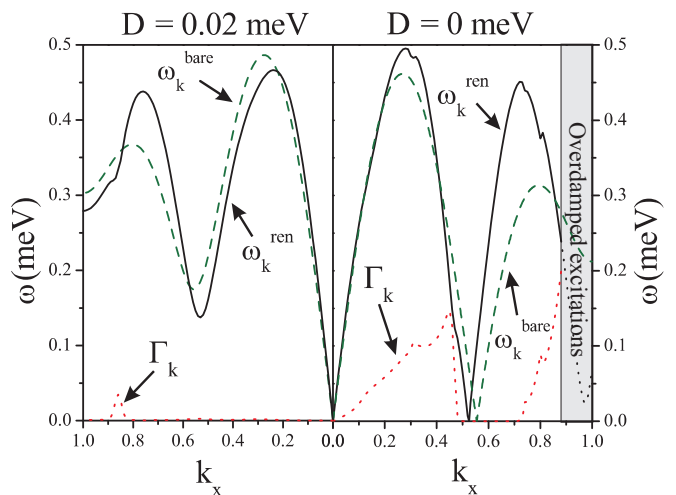


FIG. 3: (Color Online) The two panels present the results for the bare and renormalized energy spectra for the cases of $D = 0$ and $D = 0.02$ meV. Spin-wave energies are shown together with the inverse lifetime $\Gamma_{\mathbf{k}}$. The path in the two-dimensional Brillouin zone sweeps from (00) point to (10) . k_x , k_y are measured in units of 2π and $2\pi/\sqrt{3}$ respectively.

fluctuations, in addition to shifting Q towards π , reduce the size of the gap at this point. However, the effect of suppression of the gap towards zero, is relatively small for $D = 0.02$ meV.

VI. SCATTERING INTENSITY

In this Section, the dynamical properties of an anti-ferromagnet described by the model of Eq. (1) are calculated within the framework of the $1/(2S)$ expansion. We are specifically interested in answering the question of whether anharmonic spin waves can account for the main features seen in inelastic neutron scattering measurements on Cs_2CuCl_4 .¹⁴ We begin with expressions for the structure factor components that enter the formula for the inelastic neutron scattering cross section. These results were obtained earlier by Ohyama and Shiba,²⁹ and we simply quote them here.

Neutron scattering spectra of spin excitations in magnetic solids may be expressed in terms of the Fourier transformed real-time dynamical correlation function, $i, k = (x, y, z)$

$$S^{ik}(\mathbf{k}, \omega) = \frac{1}{2\pi} \int_{-\infty}^{\infty} dt \sum_{\mathbf{R}} \langle S_0^i(0) S_{\mathbf{R}}^k(t) \rangle e^{i(\omega t - \mathbf{k} \cdot \mathbf{R})}. \quad (63)$$

For the spiral spin density wave state, $S^{xx}(\mathbf{k}, \omega) = S^{zz}(\mathbf{k}, \omega)$. The complete expression for the inelastic, differential scattering cross-section, including polarization factors, is given by²⁷

$$I(\mathbf{k}, \omega) = p_x S^{xx}(\mathbf{k}, \omega) + p_y S^{yy}(\mathbf{k}, \omega), \quad (64)$$

$$p_x = 1 + \cos^2 \alpha_{\mathbf{k}}, \quad p_y = \sin^2 \alpha_{\mathbf{k}}, \quad (65)$$

where $\alpha_{\mathbf{k}}$ is the angle between the scattering wave vector \mathbf{k} and the axis perpendicular to the plane of the spins.

We begin by calculating the corresponding time-ordered spin-spin correlation functions in the rotated coordinate system

$$iF^{\alpha\beta}(\mathbf{k}, \omega) = \int_{-\infty}^{\infty} dt e^{-i\omega t} \langle \hat{T} S_{-\mathbf{k}}^{\alpha}(0) S_{\mathbf{k}}^{\beta}(t) \rangle, \quad (66)$$

where $\alpha, \beta = (\xi, \eta, \zeta)$ are the rotated coordinate axes given by Eqs. (5). The dynamical structure factor is related to the imaginary parts of these correlation functions in the following way:

$$S^{yy}(\mathbf{k}, \omega) = -\frac{1}{\pi} \text{Im} F^{\eta\eta}(\mathbf{k}, \omega), \quad (67)$$

$$S^{xx}(\mathbf{k}, \omega) = S^{zz}(\mathbf{k}, \omega) = -\frac{1}{\pi} \text{Im} [\Theta^+(\mathbf{k} + \mathbf{Q}, \omega) + \Theta^-(\mathbf{k} - \mathbf{Q}, \omega)], \quad (68)$$

$$S^{xz}(\mathbf{k}, \omega) = -S^{zx}(\mathbf{k}, \omega) = -\frac{i}{\pi} \text{Im} [\Theta^+(\mathbf{k} + \mathbf{Q}, \omega) - \Theta^-(\mathbf{k} - \mathbf{Q}, \omega)], \quad (69)$$

with,

$$\Theta^{\pm}(\mathbf{k}, \omega) = \frac{1}{4} \{ F^{\xi\xi}(\mathbf{k}, \omega) + F^{\zeta\zeta}(\mathbf{k}, \omega) \mp i [F^{\xi\zeta}(\mathbf{k}, \omega) - F^{\zeta\xi}(\mathbf{k}, \omega)] \}. \quad (70)$$

We treat the interactions between the magnons as a perturbation in the formally small parameter $1/(2S)$, and use the standard \hat{S} -matrix expansion while calculating the averages of the magnon operators $a_{\mathbf{k}}(t)$.²⁸ As a result,

$$\begin{aligned} F^{\eta\eta}(\mathbf{k}, \omega) &= \frac{S}{2} c_y^2 [G_{11}(\mathbf{k}, \omega) + G_{22}(\mathbf{k}, \omega) - 2G_{12}(\mathbf{k}, \omega)], \\ F^{\xi\xi}(\mathbf{k}, \omega) &= \frac{S}{2} c_x^2 [G_{11}(\mathbf{k}, \omega) + G_{22}(\mathbf{k}, \omega) + 2G_{12}(\mathbf{k}, \omega)], \end{aligned} \quad (71)$$

where the Green's function are determined from Eq. (37) with the self-energies given by Eqs. (39)-(42), and, to the relevant order in $1/(2S)$,

$$\begin{aligned} c_y &= 1 - \frac{1}{4SN} \sum_{\mathbf{k}} (2v_{\mathbf{k}}^2 - u_{\mathbf{k}}v_{\mathbf{k}}), \\ c_x &= 1 - \frac{1}{4SN} \sum_{\mathbf{k}} (2v_{\mathbf{k}}^2 + u_{\mathbf{k}}v_{\mathbf{k}}). \end{aligned} \quad (72)$$

The term that mixes the transverse and longitudinal fluctuations has the form:

$$\begin{aligned} i [F^{\xi\zeta}(\mathbf{k}, \omega) - F^{\zeta\xi}(\mathbf{k}, \omega)] &= c_x \{ P^{(1)}(\mathbf{k}, \omega) [G_{11}(\mathbf{k}, \omega) + G_{22}(\mathbf{k}, \omega) - 2G_{12}(\mathbf{k}, \omega)] \\ &\quad + P^{(2)}(\mathbf{k}, \omega) [G_{11}(\mathbf{k}, \omega) - G_{22}(\mathbf{k}, \omega)] \}. \end{aligned} \quad (73)$$

with the functions $P^{(1,2)}(\mathbf{k}, \omega)$ defined as

$$\begin{aligned} P^{(1)}(\mathbf{k}, \omega) &= \frac{S}{4N} \sum_{\mathbf{q}} \Phi^{(1)}(\mathbf{q}, \mathbf{k} - \mathbf{q}) (u_{\mathbf{q}}v_{\mathbf{k}-\mathbf{q}} + v_{\mathbf{q}}u_{\mathbf{k}-\mathbf{q}}) \left(\frac{1}{\omega_{\mathbf{q}} + \omega_{\mathbf{k}-\mathbf{q}} - \omega - i\eta} + \frac{1}{\omega_{\mathbf{q}} + \omega_{\mathbf{k}-\mathbf{q}} + \omega - i\eta} \right), \\ P^{(2)}(\mathbf{k}, \omega) &= \frac{S}{4N} \sum_{\mathbf{q}} \Phi^{(2)}(\mathbf{q}, \mathbf{k} - \mathbf{q}) (u_{\mathbf{q}}v_{\mathbf{k}-\mathbf{q}} + v_{\mathbf{q}}u_{\mathbf{k}-\mathbf{q}}) \left(\frac{1}{\omega_{\mathbf{q}} + \omega_{\mathbf{k}-\mathbf{q}} - \omega - i\eta} - \frac{1}{\omega_{\mathbf{q}} + \omega_{\mathbf{k}-\mathbf{q}} + \omega - i\eta} \right). \end{aligned} \quad (74)$$

As before, $\omega_{\mathbf{k}} = 2S\varepsilon_{\mathbf{k}}$. The longitudinal correlations expanded in inverse powers of $2S$ can be expressed as a sum of two contributions

$$F^{\zeta\zeta}(\mathbf{k}, \omega) = F_0^{\zeta\zeta}(\mathbf{k}, \omega) + F_1^{\zeta\zeta}(\mathbf{k}, \omega), \quad (75)$$

where

$$F_0^{\zeta\zeta}(\mathbf{k}, \omega) = -\frac{1}{2N} \sum_{\mathbf{q}} (u_{\mathbf{q}}v_{\mathbf{k}-\mathbf{q}} + v_{\mathbf{q}}u_{\mathbf{k}-\mathbf{q}})^2 \left(\frac{1}{\omega_{\mathbf{q}} + \omega_{\mathbf{k}-\mathbf{q}} - \omega - i\eta} + \frac{1}{\omega_{\mathbf{q}} + \omega_{\mathbf{k}-\mathbf{q}} + \omega - i\eta} \right), \quad (76)$$

$$F_1^{\zeta\zeta}(\mathbf{k}, \omega) = \frac{1}{2S} \left\{ \left(P^{(1)}(\mathbf{k}, \omega) \right)^2 [G_{11}(\mathbf{k}, \omega) + G_{22}(\mathbf{k}, \omega) + 2G_{12}(\mathbf{k}, \omega)] + \left(P^{(2)}(\mathbf{k}, \omega) \right)^2 [G_{11}(\mathbf{k}, \omega) + G_{22}(\mathbf{k}, \omega) - 2G_{12}(\mathbf{k}, \omega)] + 2P^{(1)}(\mathbf{k}, \omega)P^{(2)}(\mathbf{k}, \omega) [G_{11}(\mathbf{k}, \omega) - G_{22}(\mathbf{k}, \omega)] \right\}. \quad (77)$$

Note that the term $F_1^{\zeta\zeta}(\mathbf{k}, \omega)$ is formally of order $1/(2S)^2$ compared to the leading one magnon contributions Eq. (71). However, it is kept because it contains the self-energy corrections to Eq. (76) describing the two magnon continuum.

Using the set of formulas above, we have calculated the scattering intensities as a function of frequency for various trajectories in \mathbf{k} and ω space, corresponding to the measured spectra.¹⁴ In general our results agree with those of Veillette et al.²³ except for small differences due to their use of self-consistent energy denominators in the self-energies and our use of shifted \mathbf{Q} values in the anharmonic Green's functions. Veillette et al. restricted their attention to values of J , J' and D given by Eqs. (2)-(3). In the discussion that follows, we will also consider the consequences of varying the D parameter, which both shifts certain modes and also controls the size of quantum fluctuations, as well as varying the overall energy scale, J .

We focus our attention on two trajectories in the (\mathbf{k}, ω) space whose parameterizations correspond to the scans G and J of Ref. 14,

$$\begin{aligned} G: \quad k_x &= 0.5, \quad k_y = 1.53 - 0.32\omega - 0.1\omega^2 \\ J: \quad k_x &= 0.47, \quad k_y = 1.0 - 0.45\omega. \end{aligned} \quad (78)$$

In Eq. (78), k_x and k_y are written in the units of 2π and $2\pi/\sqrt{3}$ respectively, while the energy is measured in meV. Since the momentum transfer lies in the x - z plane, $p_x = p_y = 1$ for both of those scans. It is important also to take into account the finite energy and momentum resolution of the scattered neutrons. The finite energy resolution $\Delta\omega \approx 0.016$ meV leads to a small Lorentzian broadening of the one-magnon peaks. However, the effect of smearing due to the finite momentum resolution $\Delta k/2\pi = 0.085$ is much more pronounced and considerably broadens the structure of the G and J scans. What is special about the G and J scans is that they both exhibit sharp low-energy modes with energies around 0.1 meV. As we shall see, the energies of these peaks are quite sensitive to the exact value of the DM interaction D .

In Fig. 4, we plot the results of scattering intensity calculations for scan G, a data set which was analyzed in detail by Coldea et al.¹⁴ In particular, it was claimed that the high-energy tail in this scan has too much intensity, by nearly an order of magnitude, to be explained by linear spin-wave theory. Our calculations were done using the bare couplings J and J' , and the Dzyaloshinskii-Moriya interaction was set equal to $D = 0.02$ meV, the value obtained from experiments in high magnetic field.²⁴ The theory predicts three peaks, one corresponding to the principal mode $\varepsilon_{\mathbf{k}}$ and the other two, reflecting the

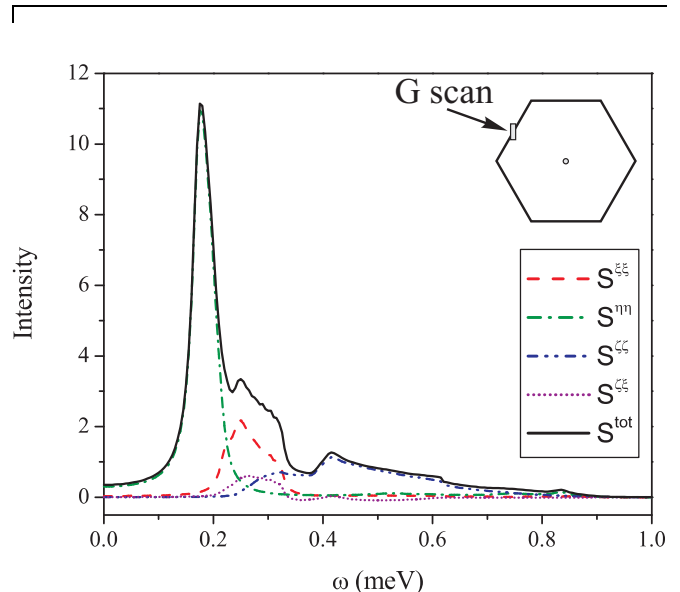


FIG. 4: (Color Online) Intensity of the scattered neutrons for scan G in Eq. (78), in the presence of Dzyaloshinskii-Moriya interaction $D = 0.02$ meV. The energy and momentum resolutions are taken to be $\Delta\omega = 0.016$ meV and $\Delta k = 0.085$ respectively. The thick solid line is the total scattering intensity, Eq. (64). Other lines represent the various contributions appearing in Eqs. (67)-(71).

presence of the shifted secondary spin waves at $\varepsilon_{\mathbf{Q}\pm\mathbf{k}}$. For the non-renormalized couplings J and J' , Eq. (24) for the bare spectrum predicts that the principal peak should be at 0.22 meV while the secondary peaks are very close to each other and located approximately at energy 0.28 meV. Inclusion of self-energies to order $1/(2S)$ renormalizes the position of the main peak down to 0.18 meV. The principal one-magnon peak should lie below a two-magnon scattering continuum starting exactly at the location of the principal peak. However, the presence of self-energies in the Green's functions, leads to a shift in positions of their poles, and to a finite gap between the principal peak and the start of the two magnon scattering continuum. This result is an artifact of truncating the perturbation expansion at a finite order, as discussed by Veillette et al.²³ We also observe that the two secondary peaks are so close to each other that it is difficult to distinguish them, once the finite frequency and momentum resolution is fully incorporated into the calculations. Experimentally, the main peak is observed at a somewhat smaller energy of 0.107 meV, while the secondary ones are located around 0.25 meV.¹⁴ Fig. 4 also shows the sign and magnitude of the various contributions to the total intensity. It is seen that the two-magnon part, integrated over the full range of frequencies, carries a considerable

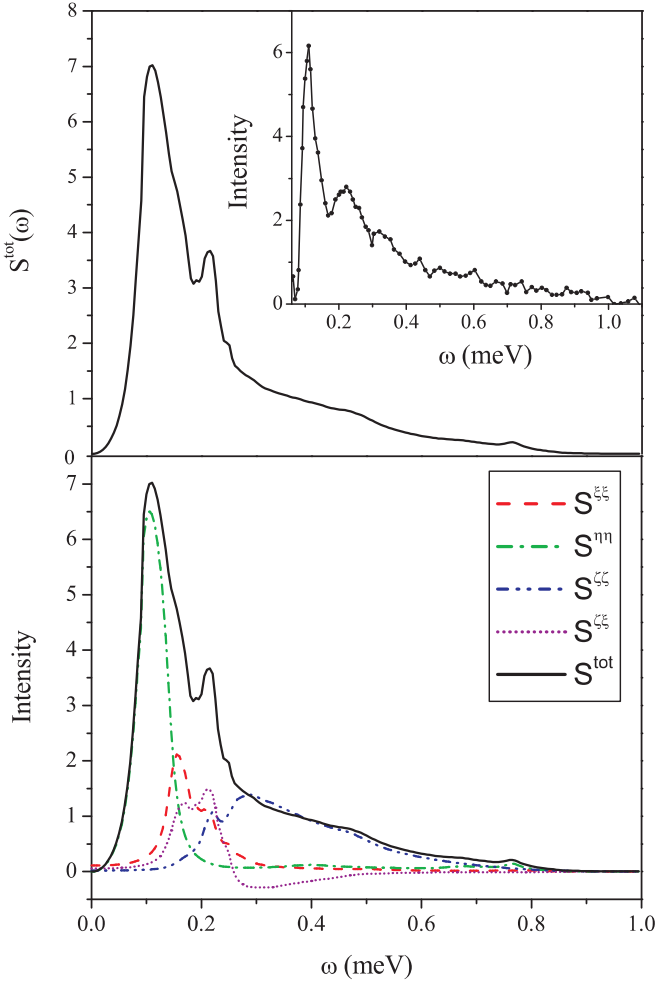


FIG. 5: (Color Online) Intensity of the scattered neutrons corresponding to scan G, for the value of Dzyaloshinskii-Moria interaction $D = 0.01$ meV. *Upper panel:* The total structure factor with the energy (momentum) resolution $\Delta E = 0.016$ meV ($\Delta k = 0.085$). *Inset:* Experimental data from Ref. 14. *Lower panel:* Different components which contribute to the structure factor (see Eqs. (67)-(71) in the text).

overall weight compared to the one-magnon contribution. At the same time, the term mixing the transverse and longitudinal fluctuations can have both signs, and being small, does not influence the intensity profile very much.

Why is the two-magnon intensity in our calculation so much larger, relative to the principal peak than in the analysis of Coldea et al.? The reason is the factor c_y^2 which renormalizes the out-of-plane scattering and which is basically due to the reduction of the local moment by quantum fluctuations. As noted above, theory predicts a much smaller local moment than the surprisingly large value obtained from experiment.³¹ According to our calculations, the moment reduction increases with decreasing D , and the ordered moment vanishes for $D < 0.003$ meV.

In Fig. 5, we plot the theoretical result for scan G, but this time with a reduced DM interaction $D = 0.01$ meV.

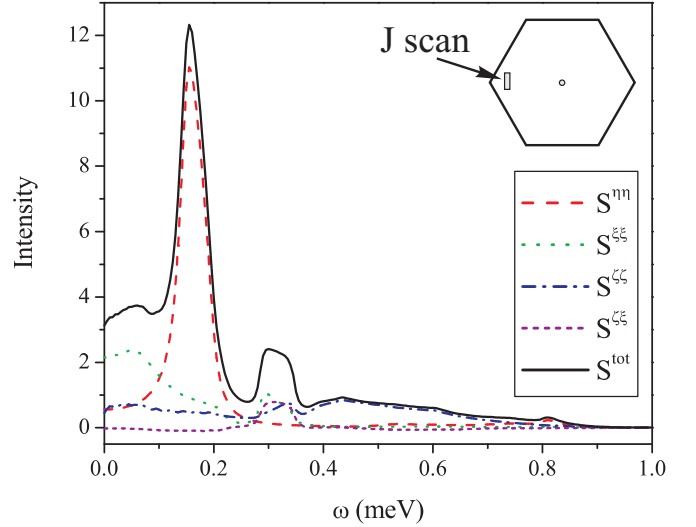


FIG. 6: (Color Online) Intensity of the scattered neutrons corresponding to scan J, Eq. (78), in the presence of Dzyaloshinskii-Moria interaction $D = 0.02$ meV. The different components are displayed as in Figs. 4, 5

The comparison of our calculations with the experimental measurements reported in Ref. 14, is displayed in the upper panel. We see that for this value of D , the position of the principal magnon peak is shifted towards smaller energies. The gap between the main peak and the energy where the continuum appears, is also decreased; there is further broadening of the principal peak and more intensity in the two-magnon continuum. It appears that the value $D = 0.01$ meV provides a better explanation of the form of the total scattering intensity for scan G than $D = 0.02$ meV. Comparison of the plots for a range of values of D , shows that the scattering intensity is very sensitive to the strength of the DM interaction. [Note that the DM interaction was not included in the analysis of Ref. 14.] Finally, we observe that even this smaller value of $D = 0.01$ meV does not account for all of the high energy scattering which seems to extend up to 1 meV, suggesting additional correlations at high energy which are not contained in the theory.

Next, we examine scan J which probes the vicinity of the ordering wave vector.¹⁴ Inelastic scattering at this point should show a primary peak at the wave vector $\mathbf{k}_J \approx \mathbf{Q}$ and two secondary modes, corresponding to momentum transfer $\mathbf{k}_J \pm \mathbf{Q}$. The primary mode, which is prominent in the theoretical spectrum, directly measures the strength of the DM interaction, since its energy is proportional to \sqrt{DJ} . The experimental data for point J, shown only in the inset of Fig. 5G in the paper of Coldea and co-workers,¹⁴ do not extend to low enough energy to display this peak. Nevertheless the position of the peak, at an energy of 0.10(1) meV, is listed in Table 1 of that paper. This value of the mode at the J point is noticeably smaller than anharmonic spin-wave theory would predict for $D = 0.02$ meV, suggesting that

the effective value of the DM interaction constant D is smaller than 0.02 meV. Since the theory, for $D = 0.02$ meV, gives a peak at 0.15 meV, a fit to the measured peak at 0.1 meV would suggest a value of D in the range of 0.008 to 0.01 meV. Of the two secondary peaks at the J point, one has an energy close to zero, corresponding to the shifted zone-center mode, while the other lies at higher energy, just above 0.3 meV.

VII. DISCUSSION AND CONCLUSIONS

The main motivation for the work presented in this paper was to see if a relatively conventional anharmonic spin-wave calculation could account for neutron scattering measurements on Cs_2CuCl_4 . Our conclusion is a qualified “yes”.

Without any calculations, one knows that the observed excitations are from an ordered state exhibiting magnetic Bragg peaks, and hence that the lowest-lying excitations must be spin waves. However, both linear and anharmonic spin-wave theory suggest a substantial moment reduction for a broad range around the expected values of D/J and J'/J . Further experiments would be useful to verify the amount by which the moment is reduced, since the present result³¹ is inconsistent both with anharmonic spin-waves and with close proximity to a spin-liquid state.

At low energies we find that we can fit the sharp spin-wave features of the data, albeit with a somewhat smaller value of the DM interaction constant, D , than was obtained from high field measurements of a fully polarized state. We also find from theoretical calculations that, without a sufficiently large DM interaction, long range order is destroyed by quantum fluctuations. However, the value of D that best fits theory to experiment is well within the range in which order is stable, at least for $T = 0$. Additional experiments, including measurements of the renormalized D in zero field, might clarify this point. (We note in passing that a value of J about 30-40% larger than given by Eq. (2), for fixed J'/J , would provide a much improved fit to the higher energy one-spin-wave features.)

Our theory yields a considerable amount of continuous two-spin-wave scattering. However the amount of this scattering, although readily measurable, is somewhat less than is observed experimentally. Furthermore, calculation of the relative size of one- and two-spin-wave features is complicated by their sensitivity to the size of D . That is, a smaller D suppresses one-spin-wave scattering and makes two-spin-wave continuous scattering relatively more conspicuous. Quantum fluctuations also broaden the one-spin-wave features via lifetime effects. However, it is difficult to assess, from the data alone, how much of the observed broadening of the principal peaks is due to lifetimes and how much is due to low momentum resolution as was emphasized by Veillette et al.²³ The theory suggests though that experiments with higher momen-

tum resolution are likely to reveal considerably sharper low energy spin-wave peaks.

With regard to the shape of the broad scattering at higher energies, we are inclined toward a picture of scattering by quasi-one-dimensional spinons. With a bare interchain coupling of 0.128 meV, which we know to be considerably renormalized downward by quantum fluctuations, one might expect that, at energies above about 0.3 meV, the system would behave like a collection of uncoupled chains. In this sense we would expect the high-energy response of the system to be better described by one-dimensional spinons than by a low-order spin-wave perturbation calculation such as the one that we have studied.

Acknowledgments

This project has been supported by the Natural Sciences and Engineering Research Council (NSERC) of Canada and by the Canadian Institute for Advanced Research (CIAR). The authors gratefully acknowledge valuable discussions and correspondence with Martin Veillette, who also provided access to a particularly useful computer program. Some of the research for this paper was done at the Aspen Center for Physics.

APPENDIX A: $1/(2S)^2$ CORRECTION TO THE GROUND STATE ENERGY AND ORDERING WAVE VECTOR

The ground state energy correction at the order $1/(2S)^2$, denoted here as $E_G^{(2)}(Q)$, consists of two parts,

$$E_G^{(2)}(Q) = \mathcal{E}_3(Q) + \mathcal{E}_4(Q). \quad (\text{A1})$$

$\mathcal{E}_4(Q)$ is obtained simply by substituting the Bogoliubov transformation Eq. (22) into $\mathcal{H}^{(4)}$ and performing the normal ordering in the terms containing two pairs of quasiparticle operators c and c^\dagger . In this Appendix, we present the results of calculations in which the Dzyaloshinskii-Moria interaction $D = 0$, so that

$$\mathcal{E}_4(Q) = \frac{1}{2N} \sum_{\mathbf{k}} \left[\varepsilon_{\mathbf{k}} \left(1 - \frac{1}{N} \sum_{\mathbf{p}} \frac{A_{\mathbf{p}}}{\varepsilon_{\mathbf{p}}} \right) - \frac{A_{\mathbf{k}}}{2} \right] + \frac{1}{N^2} \sum_{\mathbf{k}, \mathbf{p}} (A_{\mathbf{k}-\mathbf{p}} - B_{\mathbf{k}-\mathbf{p}}) \frac{A_{\mathbf{k}} A_{\mathbf{p}} + B_{\mathbf{k}} B_{\mathbf{p}}}{4\varepsilon_{\mathbf{k}} \varepsilon_{\mathbf{p}}}. \quad (\text{A2})$$

$\mathcal{E}_3(Q)$ ensues due to the key role of the cubic interactions (19) in the total Hamiltonian. It is technically advantageous first to express (19) in terms of the quasiparticle c -operators, so that

$$\mathcal{H}^{(3)} = \frac{i}{2} \sqrt{\frac{S}{2N}} \sum_{\mathbf{1}, \mathbf{2}, \mathbf{3}} \left\{ \frac{1}{3} \Gamma_1(\mathbf{1}, \mathbf{2}, \mathbf{3}) \left(c_3 c_2 c_1 - c_1^\dagger c_2^\dagger c_3^\dagger \right) + \Gamma_2(\mathbf{1}, \mathbf{2}, \mathbf{3}) \left(c_3^\dagger c_2 c_1 - c_1^\dagger c_2^\dagger c_3 \right) \right\}, \quad (\text{A3})$$

$$\begin{aligned} \Gamma_1(\mathbf{1}, \mathbf{2}, \mathbf{3}) &= (C_1 + C_2)(u_1 u_2 v_3 + v_1 v_2 u_3) && + (C_2 - C_3)(u_1 v_2 u_3 + v_1 u_2 v_3). \quad (\text{A5}) \\ &+ (C_1 + C_3)(u_1 u_3 v_2 + v_1 v_3 u_2) \\ &+ (C_2 + C_3)(u_2 u_3 v_1 + v_2 v_3 u_1), \quad (\text{A4}) \end{aligned}$$

$$\begin{aligned} \Gamma_2(\mathbf{1}, \mathbf{2}; \mathbf{3}) &= (C_1 + C_2)(u_1 u_2 u_3 + v_1 v_2 v_3) \\ &+ (C_1 - C_3)(v_1 u_2 u_3 + u_1 v_2 v_3) \end{aligned}$$

At $T = 0$, the only contribution to $\mathcal{E}_3(Q)$ is given by the 'sunrise' diagram containing two vertices $\Gamma_1(\mathbf{q}, \mathbf{p}, -\mathbf{q} - \mathbf{p})$. Using the formulas (23), we arrive at the following expression for \mathcal{E}_3 :

$$\begin{aligned} \mathcal{E}_3(Q) &= -\frac{1}{24N^2} \sum_{\mathbf{p}, \mathbf{q}} \frac{[\Gamma_1(\mathbf{q}, \mathbf{p}, -\mathbf{q} - \mathbf{p})]^2}{\varepsilon_{\mathbf{p}} + \varepsilon_{\mathbf{q}} + \varepsilon_{\mathbf{p}+\mathbf{q}}} = -\frac{1}{16N^2} \sum_{\mathbf{p}, \mathbf{q}} \frac{1}{(\varepsilon_{\mathbf{p}} + \varepsilon_{\mathbf{q}} + \varepsilon_{\mathbf{p}+\mathbf{q}})} \left\{ C_{\mathbf{p}+\mathbf{q}}^2 \left(\frac{A_{\mathbf{p}+\mathbf{q}} + B_{\mathbf{p}+\mathbf{q}}}{\varepsilon_{\mathbf{p}+\mathbf{q}}} \right) \left(\frac{A_{\mathbf{p}} A_{\mathbf{q}} + B_{\mathbf{p}} B_{\mathbf{q}}}{\varepsilon_{\mathbf{p}} \varepsilon_{\mathbf{q}}} - 1 \right) \right. \\ &\quad \left. + C_{\mathbf{p}} C_{\mathbf{q}} \left[\frac{(A_{\mathbf{p}+\mathbf{q}} + B_{\mathbf{p}+\mathbf{q}})(A_{\mathbf{p}} + B_{\mathbf{p}})(A_{\mathbf{q}} + B_{\mathbf{q}})}{\varepsilon_{\mathbf{p}+\mathbf{q}} \varepsilon_{\mathbf{p}} \varepsilon_{\mathbf{q}}} + \frac{A_{\mathbf{p}+\mathbf{q}} - B_{\mathbf{p}+\mathbf{q}}}{\varepsilon_{\mathbf{p}+\mathbf{q}}} - \frac{A_{\mathbf{p}} + B_{\mathbf{p}}}{\varepsilon_{\mathbf{p}}} - \frac{A_{\mathbf{q}} + B_{\mathbf{q}}}{\varepsilon_{\mathbf{q}}} \right] \right\}. \quad (\text{A6}) \end{aligned}$$

Numerical calculations show that for the interaction constants given by Eqs. (2),

$$\mathcal{E}_3(Q_0)/J = -0.0425, \quad (\text{A7})$$

$$\mathcal{E}_4(Q_0)/J = 0.0103, \quad (\text{A8})$$

which are quite small. The $1/(2S)^2$ correction to Q_0 can be computed by substituting the expansion

$$Q = Q_0 + \frac{\Delta Q^{(1)}}{2S} + \frac{\Delta Q^{(2)}}{(2S)^2} \quad (\text{A9})$$

into the series for the ground state energy

$$E_G(Q) = S^2 J_{\mathbf{Q}} + S E_G^{(1)}(Q) + E_G^{(2)}(Q), \quad (\text{A10})$$

and expanding its minimum in powers of $1/(2S)$. As a result,

$$\Delta Q^{(2)} = - \left[\frac{\partial^2 J_{\mathbf{Q}}}{\partial Q^2} \right]^{-1} \cdot \left[\frac{1}{2} \frac{\partial^3 J_{\mathbf{Q}}}{\partial Q^3} \cdot (\Delta Q^{(1)})^2 \right]$$

$$+ 2 \frac{\partial^2 E_G^{(1)}(Q)}{\partial Q^2} \cdot (\Delta Q^{(1)}) + 4 \frac{\partial E_G^{(2)}(Q)}{\partial Q} \Bigg|_{Q_0} \quad (\text{A11})$$

The calculations of derivatives over Q in expressions entering Eqs. (26), (A6), (A2) are lengthy but straightforward. Omitting the corresponding cumbersome final expressions, we state here that as a result of numerical integration:

$$\Delta Q^{(2)}/2\pi \approx -0.011. \quad (\text{A12})$$

The value of the ground state energy at its minimum ($S = 1/2$)

$$E_{min}/J = \frac{1}{J} \left[S^2 J_{\mathbf{Q}} + S E_G^{(1)}(Q) + E_G^{(2)}(Q) - \frac{1}{8} \frac{\partial^2 J_{\mathbf{Q}}}{\partial Q^2} \cdot (\Delta Q^{(1)})^2 \right] \Bigg|_{Q_0} = -0.459. \quad (\text{A13})$$

Note that the last term in Eq. (A13) is always negative and arises solely due to the shift in the ordering wave vector $\Delta Q^{(1)}$. Numerically however, this term is tiny, even compared to the second order correction $E_G^{(2)}(Q_0)$ that itself gives a small contribution to the total energy Eq. (A13).

¹ See T. Senthil, cond-mat/0411275, and references therein.

² P. W. Anderson, Mater. Res. Bull. **8**, 153 (1973); P. Fazekas

- and P. W. Anderson, *Philos. Mag.* **30**, 23 (1974).
- ³ S. A. Kivelson, D. S. Rokhsar, and J. P. Sethna, *Phys. Rev. B* **35**, 8865 (1987).
 - ⁴ A. O. Gogolin, A. A. Nersesyan and A. M. Tsvelik, *Bosonization in Strongly Correlated Systems* (Cambridge University Press, Cambridge, 1999).
 - ⁵ See, e. g., *Perspectives in Quantum Hall Effects: Novel Quantum Liquids in Low-Dimensional Semiconductor Structures*, Ed. by S. Das Sarma and A. Pinzucuk (Wiley, New York, 1996).
 - ⁶ R. Moessner and S.L. Sondhi, *Phys. Rev. Lett.* **86**, 1881 (2001).
 - ⁷ C. Nayak and K. Shtengel, *Phys. Rev. B* **64**, 064422 (2001).
 - ⁸ L. Balents, M. P. A. Fisher, and C. Nayak, *Int. J. Mod. Phys. B* **12**, 1033 (1998).
 - ⁹ L. Balents, M. P. A. Fisher, and C. Nayak, *Phys. Rev. B* **60**, 1654 (1999).
 - ¹⁰ L. Balents, M. P. A. Fisher, and C. Nayak, *Phys. Rev. B* **61** 6307 (2000).
 - ¹¹ E. Demler, C. Nayak, H.-Y. Kee, Y. B. Kim, and T. Senthil, *Phys. Rev. B* **65**, 155103 (2002).
 - ¹² T. Senthil and O. Motrunich, *Phys. Rev. B* **66**, 205104 (2002); O. I. Motrunich and T. Senthil, *Phys. Rev. Lett.* **89**, 277004 (2002).
 - ¹³ L. Balents, M.P.A. Fisher and S.M. Girvin, *Phys. Rev. B* **65**, 224412 (2002).
 - ¹⁴ R. Coldea, D. A. Tennant and Z. Tylczynski, *Phys. Rev. B* **68**, 134424 (2003).
 - ¹⁵ R. Coldea, D. A. Tennant and Z. Tylczynski, *Phys. Rev. Lett.* **86**, 1335 (2001).
 - ¹⁶ Z. Weihong, R. H. McKenzie and R. R. P. Singh, *Phys. Rev. B* **59**, 14367 (1999).
 - ¹⁷ W. Zheng, J. O. Fjaerestad, R. R. P. Singh, R. H. McKenzie, and R. Coldea, *cond-mat/0506400*.
 - ¹⁸ C. H. Chung, J. B. Marston and R. H. McKenzie, *J. Phys.: Condens. Matter* **13**, 5159 (2001); S. Takei, C. H. Chung and Y. B. Kim, *Phys. Rev. B* **70**, 104402 (2004).
 - ¹⁹ Y. Zhou and X. G. Wen, *cond-mat/0210662*.
 - ²⁰ C.-H. Chung, K. Voelker, and Y. B. Kim, *Phys. Rev. B* **68**, 094412 (2003).
 - ²¹ J. Merino, Ross H. McKenzie, J. B. Marston and C. H. Chung, *J. Phys.: Condens. Matter* **11**, 2965 (1999).
 - ²² J. Alicea, O. I. Motrunich, M. P. A. Fisher, *cond-mat/0512427*.
 - ²³ M. Y. Veillette, A. J. A. James, and F. H. L. Essler, *Phys. Rev. B* **72**, 134429, (2005).
 - ²⁴ R. Coldea, D. A. Tennant, K. Habicht, P. Smeibidl, C. Wolters and Z. Tylczynski, *Phys. Rev. Lett.* **88**, 137203(2002).
 - ²⁵ T. Holstein and H. Primakoff, *Phys. Rev.* **58**, 1098 (1940).
 - ²⁶ Y. Tokiwa, T. Radu, R. Coldea, H. Wilhelm, Z. Tylczynski, and F. Steglich, *cond-mat/0601272* (2006).
 - ²⁷ S. W. Lovesey, in *Theory of Neutron Scattering from Condensed Matter*, (Clarendon, Oxford, England, 1987).
 - ²⁸ See, e.g., A. A. Abrikosov, L. P. Gorkov & I. E. Dzyaloshinski. *Methods of Quantum Field Theory in Statistical Physics*, (Dover, New York, 1975)
 - ²⁹ T. Ohyama and H. Shiba, *J. Phys. Soc. Jpn.* **62**, 3277 (1993).
 - ³⁰ A. V. Chubukov, S. Sachdev, and T. Senthil, *J. Phys.: Condens. Matter* **6**, 8891 (1994).
 - ³¹ R. Coldea, D.A. Tennant, R.A. Cowley, D.F. McMorrow, B. Dorner, and Z. Tylczynski, *J. Phys.: Condens. Matter* **8**, 7473 (1996).